

Infusion Doping for USJ Formation

John Hautala¹, John Borland², Martin Tabat¹ and Wes Skinner¹

¹Epion Corporation, 37 Manning Road, Billerica, MA 01821, USA

²J.O.B. Technologies, 5 Farrington Lane, South Hamilton, MA 01982, USA

Tel:+1-978-215-6238, Fax:+1-978-670-9119, Email: jhautala@epion.com

Abstract

We report for the first time results on infusion doping of boron for ultra shallow junctions (USJ). Using B_2H_6 or BF_3 source gas, the resulting USJ boron dopant profile measured by SIMS shows no evidence of channeling with extreme abruptness of $<2.5\text{nm/decade}$ for a 12nm shallow junction. Infusion doping shows a power log to the 1/3 relationship between energy to junction depth in contrast to the traditional linear fit observed with ion implantation due to nuclear stopping power effects. Boron surface doping levels of $1-2E22/\text{cm}^3$ for $2E16/\text{cm}^2$ doses were achieved. Dopant activation using low temperature furnace annealing from 450°C to 950°C were compared using standard 4PP and non-penetrating elastic material 4PP for sheet resistance measurements on these USJ structures. Also, electrically active dopant profiling was conducted using spreading resistance profile (SRP) for USJ junction depth (X_j) comparison to SIMS. Use of amorphizing implantation resulted in lower R_s values after low temperature SPE annealing.

1. Introduction

Unlike ion implantation, which involves a single ionized atom, gas molecular cluster ions contain typically >5000 atoms per charge. Infusion doping of Si with Gas Cluster Ion Beam (GCIB) has been studied with a standard 300mm Epion 400 microAmp GCIB tool, shown schematically in Fig. 1, by producing clusters made up of Ar and B containing molecules such as B_2H_6 and BF_3 . In this tool, the gas cluster beam is generated by the expansion of high pressure gas through a nozzle into the vacuum. Electron impact ionization is used to ionize the clusters. After acceleration monomers are separated from the cluster beam by a transverse magnetic field. Finally, the cluster beam is neutralized to prevent substrate charging. Substrates are mechanically scanned in two dimensions to provide uniform processing of the substrates.

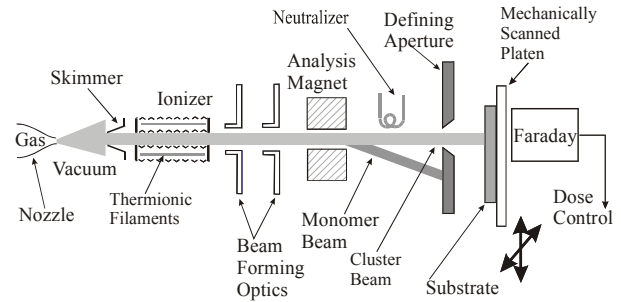


Fig. 1: Schematic of Epion's infusion doping equipment.

The gas cluster ions used for surface processing are accelerated through potentials of a few thousand volts. Although the gas cluster ions have high total energy, the energy is shared by the large number of atoms comprising the cluster, so that the energy per atom is $<10\text{eV}$. Upon impact with the silicon surface, the atoms in the gas cluster are only able to penetrate through a few atomic layers of the surface, because of the low energy per atom. This is much shallower than in the case of conventional ion implantation and allows processing effects to be confined to much shallower depths. The high total energy of the cluster ion is infused into a very small region of the silicon surface resulting in momentary surface temperature and pressure conditions which are significantly higher than those produced by conventional ion processes.

Nearly all gases and mixtures of gases can be nucleated into clusters [1-3]. Rare gases such as Ar and Xe readily form clusters as do most diatomics (ie. O_2 , N_2) and molecules (ie. B_2H_6 , BF_3 , CH_4 , NF_3 , CF_4). The kinetic removal rates are low for GCIB processing with non-reactive gases (such as Ar and B_2H_6); however, significant localized chemical effects can take place when reactive gas molecules such as CF_4 , NF_3 , O_2 , H_2 , etc. are included in the clusters and under these processing conditions, infusion surface etching will occur. The comparison of inert versus chemical GCIB etch rates of Si is shown in Fig. 2. As a consequence of the locally high temperatures in the impact infusion volume, such gas cluster beams can be used to perform well-controlled non-damaging directional chemistry on the substrate surface. This

characteristic of GCIB has been successfully used in uniform etching of SOI substrates to attain uniform fully depleted thickness [4].

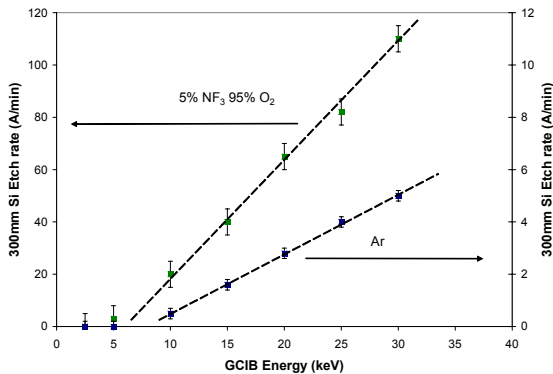


Fig. 2: Infusion surface etching results for Ar and O_2/NF_3 mixtures.

2. Infusion Surface Doping

A comparison between traditional ion implantation doping using 500eV B_{11} monomer and infusion doping by 5keV gas clusters made up of a mixture of B_2H_6 and Ar gases is shown in Fig. 3. No channeling is observed using the infusion doping technique and a $1E18/cm^3$ junction depth (X_j) at 12nm is achieved. Significant channeling can be seen with the ion implantation process resulting in an X_j at 37nm. Pre-amorphizing implantation would be required to reduce X_j to 15nm and a 300eV implant would be needed to realize an X_j at 12nm [5]. Fig. 4 shows the effects of infusion doping energy on junction depth and a realized surface boron level of $2E22/cm^3$ could be achieved with a dose of $2E16/cm^2$. Fig. 5 shows the relationship of junction depth measured at $5E19/cm^3$ versus infusion doping energy over the energy range of 2.5keV to 30keV. Unlike ion implantation, the stopping distance for infusion doping follows the energy of acceleration to the 1/3 power. This is because upon impact with the substrate, the cluster locally heats a volume of Si by a transient thermal spike (TTS). At the instant of contact with the cluster, the solids incorporated in the cluster are infused into this heated/pressurized zone. The TTS propagates in 3-dimensions and is quickly quenched. The effects of this pressurized TTS can also be seen in Fig. 6 for the case of a wafer that had a 500eV boron ion implantation (Fig. 3) followed by Ar gas cluster processing over the energy range 2.5keV to 30keV. Taking the X_j values at $5E19/cm^3$ versus the Ar cluster energy, the data follows the energy to the 1/3 results in Fig. 5. The doping process appears to be linear and

easily controllable. Fig. 7 shows the one-to-one correlation between the gas cluster dose and the SIMS measured retained boron dose in silicon.

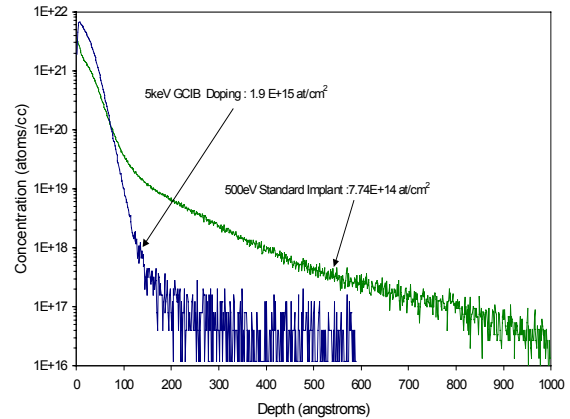


Fig. 3: SIMS comparison of implantation (channeling) and infusion (non-channeling) doping profiles.

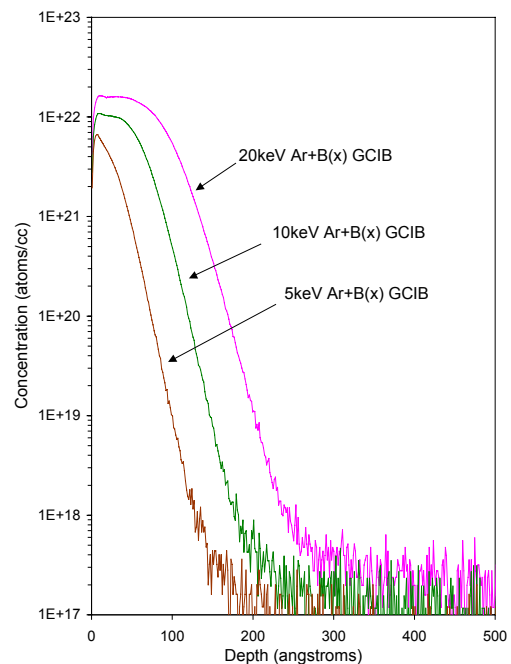


Fig. 4: SIMS dopant profiles for 5-20keV infusion doping energies.

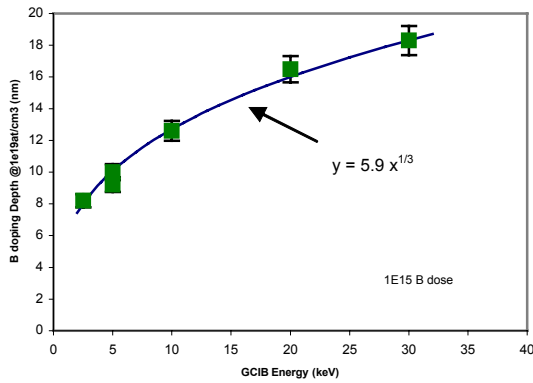


Fig.5: Infusion doping energy versus junction depth with a 1/3 power relationship.

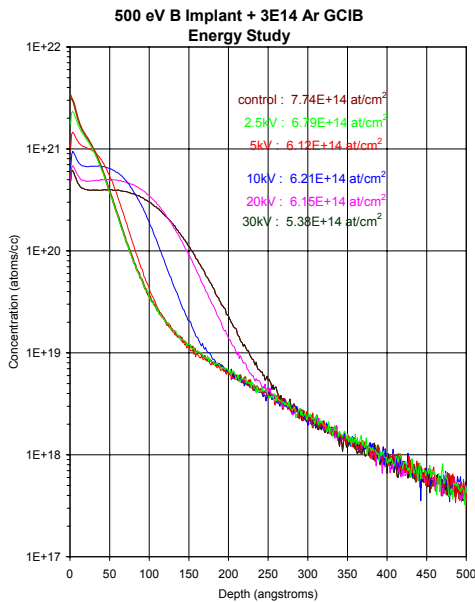


Fig. 6: Transient thermal spike localized heating effects on ion implanted boron dopant movement after various Ar gas cluster processing.

Infusion doping also has the ability to have high efficiencies. Greater than 200 B atoms can be infused into the Si for every cluster ion for a given gas mixture. In this manner, it has been demonstrated that infusion

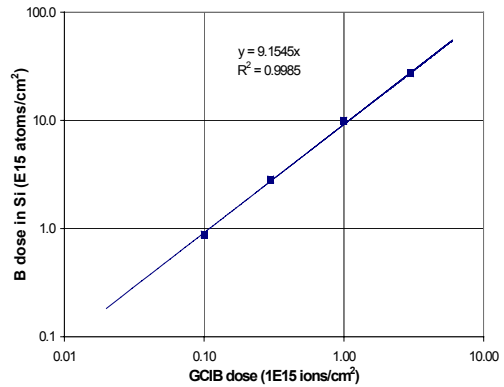


Fig. 7: Dose correlation between gas cluster dose and the SIMS measured retained dose in silicon.

doping can easily deliver >20mA of B atoms and keep the B atoms to <20nm from the surface. Initial results for an infusion doping process realizing an Xj=15nm has demonstrated a 1E15/cm² dose throughput of >100wph for 300mm wafers and at Xj=10nm a throughput >30wph.

3. Infusion Doping USJ Characterization

Various dopant activation annealing techniques were investigated including Flash/RTA up to 1250°C and furnace annealing between 550°C-950°C. The 5keV infusion doping process resulted in <14nm junctions determined by SIMS for sample 6 (Fig. 8, plot b) and <45nm for sample 5 (Fig. 8, plot c & d). With diffusion-less activation annealing the electrical Xj was <5nm as measured by SRP (sample 5) and shown in Fig. 8. Thermoelectric probe type testing confirmed p-type surface dopant conversion and EM-4PP (non-penetrating probes) measurements verified probe junction penetration when using standard 4PP as shown by the Rs data in Figs. 9 & 10. Si and Ge amorphous implants were used to improve dopant activation by SPE at 550°C. Samples 1,3 & 5 had Si amorphizing implantation at 30keV/1E15/cm² to enhance low temperature SPE dopant activation while samples 2, 4 & 6 were non-amorphous crystalline samples [5]. The Rs-vs-Xj infusion doping results for samples 5 & 6 are plotted in Fig. 11 using EM-4PP for Rs measurements and both SIMS & SRP for Xj measurements. After the 550°C SPE anneal, the Rs value for sample 5 was ~350ohms/sq. but the Xj determined by SIMS was 45nm while by SRP it was 5nm. These results clearly shows the issues with 4PP Rs measurements and SIMS junction depth measurements on electrical junctions <20nm [6].

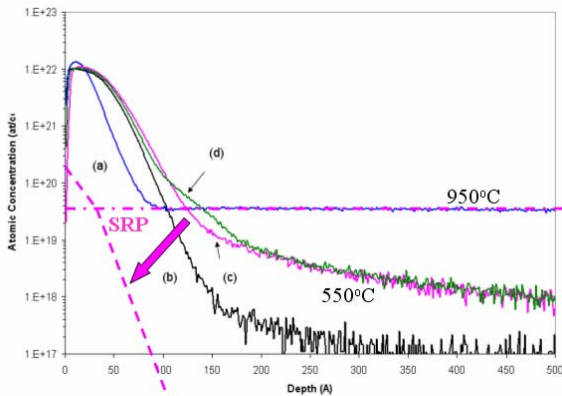


Fig. 8: SIMS-vs-SRP boron dopant profile for 550°C (b,d) and 950°C (a) annealed samples 5 (a,c,d) & 6 (a,b).

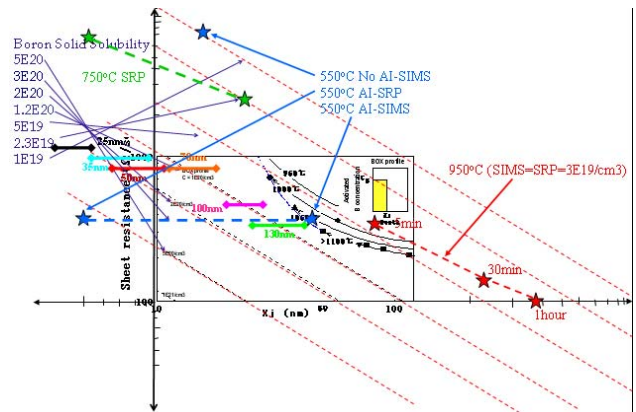


Fig. 11: Rs-vs-Xj summary results from infusion doping.

4. Summary

USJ formation using infusion doping with boron achieved <12nm junctions with a 1/3 power log relationship with no evidence of channeling and abruptness of <2.5nm/decade. Surface boron chemical doping levels as high as 2E22/cm3 were achieved. Using SRP, the electrical junction depth was 5nm with an Rs of 350ohms/sq. measured by EM-4PP for a 550°C SPE diffusion-less activation anneal. Infusion doping technique seems promising for scaling USJ down to <5nm.

Acknowledgements

The authors are grateful to Solid State Measurements for EM-4PP and SRP analysis of the infusion doping samples. Also to Vortek Industries for Flash/RTA sample annealing.

References

- [1] M. Saito, N. Toyoda, N. Hagiwara, J. Matsuo and I. Yamada, *Ion Implantation Technology-98*, 1226, edited by J. Matsuo, G. Takaoka and I. Yamada, IEEE, Piscataway (1999)
- [2] N. Toyoda, J. Matsuo and I. Yamada, *Implantation Technology-96*, 808, edited by E. Ishida, S. Banerjee, S. Mehta, T. C. Smith, M. Current, L. Larson and A. Tasch, IEEE, Piscataway (1997)
- [3] R. P. Torti, unpublished.
- [4] L. P. Allen, S. Caliendo, N. Hofmeister, E. Harrington, M. Walsh, M. Tabat, T. G. Tetreault, E. Degenkolb, C. Santeufemio and W. Skinner, *2002 IEEE International SOI Conference*, Williamsburg, VA, October 7-11 (2002).
- [5] J. Borland, T. Matsuda and K. Sakamoto, *Solid State Technology*, vol. 45, no. 6, p. 83, June 2002.
- [6] R. Hillard, J. Borland and C.W. Ye, *IWJT-2004*, to be published.

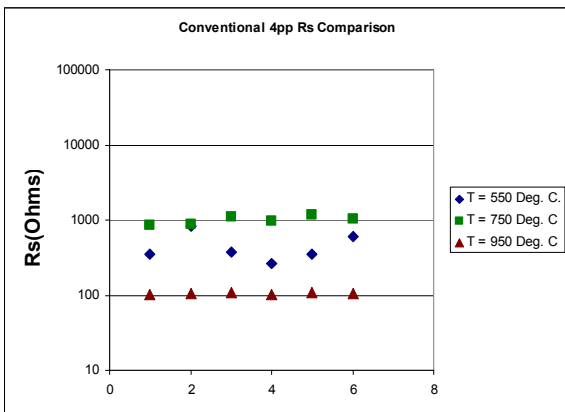


Fig. 9: Conventional 4PP measurement results.

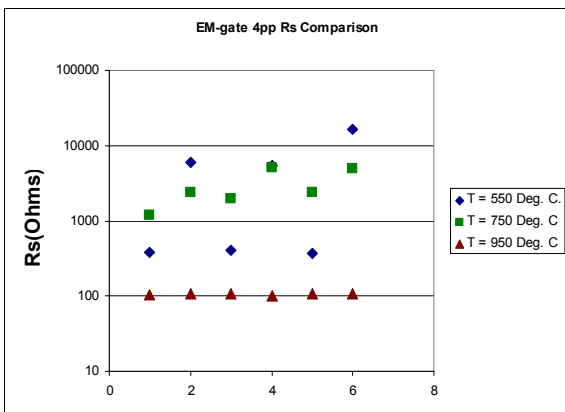


Fig. 10: EM-4PP measurement results.